

## RESEARCH ARTICLE

# The Effect of Pervasive Computing and Driver's Memory on Connected and Autonomous Vehicles

CHEN CAN<sup>1,2</sup> AND DU ZHIGANG<sup>1</sup><sup>1</sup>School of Transportation and Logistics Engineering, Wuhan University of Technology, Wuhan 430063, China<sup>2</sup>School of Civil and Environmental Engineering, Nanyang Technological University, Singapore 639798

Corresponding author: Du Zhigang (zhig\_du7@163.com)

This work was supported by the National Natural Science Foundation of China under Grant 52072291.

**ABSTRACT** Pervasive computing techniques provides application guidance and support for intelligent transportation systems. On the basis of connected autonomous vehicles, a extended model has been proposed. This paper focuses on studying the effects of the electronic throttle and driver's memory. In order to show the influence of these two factors on the model, the extended model is studied by theoretical analysis and numerical methods. Stability conditions are obtained by adding perturbation to the linear analysis, the TDGL equation and mKdV equation are derived by nonlinear analysis, which shows that the phase change behavior of traffic jams can be described by both of them. The numerical simulation results show the correctness of the analysis results. Numerical results show that the effects of driver's memory and electronic throttle play an key role in the stability of traffic flow, which is consistent with the theoretical analysis results.


**INDEX TERMS** TDGL equation, mKdV equation, driver's memory, electronic throttle, traffic flow.

## I. INTRODUCTION

Global warming is becoming more and more serious, which is closely related to our life, it is not only endangers the balance of natural ecosystems, but also threatens human survival. There are many factors contributing to this situation. Environmental pollution is one of the causes of this situation, it has become a major global problem. The main reason comes from people who burn fossil fuels, petroleum and other chemicals. Some of them come from emissions of cars, and traffic congestion will increase emissions of exhaust gas. To alleviate environmental pollution, people have started to tackle traffic congestion and slow down environmental pollution. Therefore, a series of traffic models have been proposed to analyse and solve traffic problems and make their own contribution to the mitigation of atmospheric pollution. For example, car following model [1], [2], [3], [4], [5], [6], [7], [8], [9], [10], [11], [12], [13], [14], [15], [16], [17], hydrodynamic lattice models [18], [19], [20], [21], cellular automation models [22], [23], continuum model [24], [25], [26], [27], gas kinetic models [29], [30], [31], the car following model is a micro model, which analyzes traffic congestion

from a micro perspective by establishing a new model and taking some factors into account.

Bando et. al. [28] firstly presented the optimal velocity model (OVM), which has revealed the dynamic evolution of traffic congestion in a simple way. According to this original model, many new models have been proposed. Such as generalized force model (GFM) [32], full velocity difference model (FVDM) [33], and so on [20], [34], [35], [36], [37]. In recent years, with the development of internet technology, modern technological devices are becoming more and more sophisticated. The application of intelligent transport technology has not only made traffic smarter, but has also effectively reduced traffic congestion. In the intelligent traffic environment, the traffic information of other vehicles is integrated into the collaborative driving control by using the information and communication technology system (ICT). the representative scholars in this field include Ge, *etc.* [38], [39], [40]. Vehicle-to-Vehicle communication is a very promising technology. Sun et. al. [41] studied the delay feedback control under the V2V. The intelligent driving system under the internet of vehicles environment can acquire the driving state in front of the vehicle in real time, effectively improving the stability of traffic flow. Yu et. al. [42] considered the velocity change with memory feedback under the connected cruise control (CCC). In the actual traffic environment, When a

The associate editor coordinating the review of this manuscript and approving it for publication was Giambattista Gruosso .

traffic situation occurs, the driver usually needs a certain amount of time to react to the current situation. Cao et. al. [43] created a new model, which avoids the disadvantages of existing models that ignore the sensory buffer time.

Past reports [44], [45], [46] never have linked the stability of traffic flow to electronic throttle and driver's memory effect. According to the studies we have seen, there is no article to study both electronic throttle and driver's memory effect under an intelligent transportation system. This article combines these two factors, which is different from other's articles.

The rest of this article is arranged as follows. In Section II, an extended model is proposed which takes into account both electronic throttle and driver's memory effect, the stability of the model is analyzed and the neutral stability conditions is obtained. TDGL equation is obtained by nonlinear analysis, the mKdV equation is derived. In Section III, the theoretical results are verified by numerical simulation. In Section IV, the conclusions are drawn.

## II. METHODOLOGY

### A. THE IMPROVED MODEL AND LINEAR STABILITY ANALYSIS

Jiang et.al. [33] proposed the full velocity difference model (FVDM), The formula for this model is

$$\frac{dv_n(t)}{dt} = \alpha [V(\Delta x_n(t)) - v_n(t)] + \lambda(v_{n+1}(t) - v_n(t)) \quad (1)$$

where  $\alpha$  is the sensitivity coefficient of the driver and reciprocal to the delay time  $\tau$ .  $v_n(t)$  is the velocity of car  $n$ th at time  $t$ ,  $\Delta x_n(t) = x_{n+1}(t) - x_n(t)$  represents the headway difference between two adjacent cars.  $\Delta v_n(t) = v_{n+1}(t) - v_n(t)$  is the velocity difference between the leading car  $n + 1$  and the following car  $n$  at time  $t$ .  $V(\Delta x_n(t))$  is the optimal velocity function.  $\lambda$  is the velocity difference coefficient. Based on the full velocity difference, Li et. al. [45] proposed a car-following model for CAV vehicles based on electronic throttle angle control. The model formula is

$$\frac{dv_n(t)}{dt} = \alpha [V(\Delta x_n(t)) - v_n(t)] + \lambda(v_{n+1}(t) - v_n(t)) + \kappa(\theta_{n+1}(t) - \theta_n(t)) \quad (2)$$

where  $\kappa$  is the electronic throttle angle control coefficient,  $\theta_{n+1}(t)$  and  $\theta_n(t)$  are the electronic throttle angles of the  $n$ th car and the  $n + 1$ th car at time  $t$ , respectively.

$$\frac{dv_n(t)}{dt} = -d(v_n(t) - v_e) + c(\theta_n(t) - \theta_e) \quad (3)$$

where  $d$  and  $c$  are constants, and  $d > 0$ ,  $c > 0$ .  $v_e$  is the current steady state velocity.  $\theta_e$  is the electronic throttle angle corresponding to the current steady state velocity  $v_e$ .

$$\frac{dv_n(t)}{dt} = \alpha [V(\Delta x_n(t)) - v_n(t)] + \lambda(v_{n+1}(t) - v_n(t)) + \sum_{j=1}^m w_j(\theta_{n+j}(t) - \theta_n(t)) \quad (4)$$

where  $m$  is the first  $m$  cars, and satisfies  $m < n$ ,  $w_j$  is the weight coefficient of the electronic throttle angle difference term of front  $j$  vehicles.

$$\frac{dv_n(t)}{dt} = \alpha \left[ V \left( \frac{1}{\tau_0} \int_{t-\tau_0}^t \Delta x_n(u) du \right) - v_n(t) \right] + \lambda(v_{n+1}(t) - v_n(t)) + k_1 \sum_{j=1}^m w_j(\theta_{n+j}(t) - \theta_n(t)) \quad (5)$$

We can know by using the median theorem of integrals

$$\frac{1}{\tau_0} \int_{t-\tau_0}^t \Delta x_n(u) du = \Delta x_n(t - \tau_1) \quad \tau_1 \in [t - \tau_0, t] \quad (6)$$

where the integral of  $\Delta x_n(u)$  from  $t - \tau_0$  to  $t$  represents the continuous headway of vehicle  $n$ ,  $\tau_0$  is the memory response time of the driver,  $k_1$  is the coefficient of the electronic throttle. The optimal speed function is

$$V(\Delta x_n(t)) = \frac{v_{\max}}{2} [\tanh(\Delta x_n(t) - h_c) + \tanh(h_c)] \quad (7)$$

where  $v_{\max}$  is the maximal velocity,  $h_c$  is the safe distance, the optimal velocity function  $V(\bullet)$  is a monotonically increasing function with an upper bound and a critical point at  $\Delta x_n = h_c : V'(h_c) = 0$ . The basic idea of the optimal velocity model is that when the distance between the vehicles increases infinitely, the vehicle runs at the maximum speed, and the vehicle runs smoothly. When the distance between adjacent cars decreases, the vehicles slow down to avoid collision. For the convenience of linear analysis, Eq. (5) can be converted to

$$\frac{d^2 x_n(t)}{dt^2} = \alpha \left[ V \left( \frac{1}{\tau_0} \int_{t-\tau_0}^t \Delta x_n(u) du \right) - \frac{dx_n(t)}{dt} \right] + \lambda \left( \frac{dx_{n+1}(t)}{dt} - \frac{dx_n(t)}{dt} \right) + k_1 \sum_{j=1}^m w_j(\theta_{n+j}(t) - \theta_n(t)) \quad (8)$$

Similarly, in order to facilitate subsequent nonlinear analysis, Eq. (8) is rewritten as follows

$$\frac{d^2 \Delta x_n(t)}{dt^2} = \alpha \left[ V \left( \frac{1}{\tau_0} \int_{t-\tau_0}^t \Delta x_{n+1}(u) du - \frac{1}{\tau_0} \int_{t-\tau_0}^t \Delta x_n(u) du \right) - \frac{d \Delta x_n(t)}{dt} \right] + \lambda \left( \frac{d \Delta x_{n+1}(t)}{dt} - \frac{d \Delta x_n(t)}{dt} \right) + k_1 \sum_{j=1}^m w_j(\Delta \theta_{n+j}(t) - \Delta \theta_n(t)) \quad (9)$$

In a uniform traffic flow, all vehicles travel at a fixed distance  $h$  and an optimal velocity  $V(h)$ , then the steady state solution is

$$x_n^0(t) = hn + V(h)t, \quad h = L/N \quad (10)$$

where  $N$  is the total number of vehicles and  $L$  is the length of the road. A small disturbance  $y_n(t)$  is added to the steady state solution  $x_n^0(t)$ :  $x_n(t) = x_n^0(t) + y_n(t)$ . Substituting it into Eq. (8) yields a linear equation

$$\begin{aligned} \frac{d^2 y_n(t)}{dt^2} &= \alpha \left[ V' \left( \frac{1}{\tau_0} \int_{t-\tau_0}^t \Delta y_n(u) du \right) - \frac{d y_n(t)}{dt} \right] \\ &+ \lambda \left( \frac{d y_{n+1}(t)}{dt} - \frac{d y_n(t)}{dt} \right) \\ &+ k_1 \sum_{j=1}^m w_j (\theta_{n+j}(t) - \theta_n(t)) \end{aligned} \quad (11)$$

where  $\Delta y_n(t) = y_{n+1}(t) - y_n(t)$  and  $V'(h) = dV(\Delta x_n)dt|_{\Delta x_n=h}$ . Let's expand out  $y_n(t) = e^{ikn+zt}$ , and get the following result

$$\begin{aligned} z^2 &= \alpha \left[ V'(e^{-ik} - 1) - \tau_1 z(e^{-ik} - 1) - z \right] \\ &+ \lambda z (e^{-ik} - 1) \\ &+ \frac{k_1 z}{c} \sum_{j=1}^m w_j \left[ z e^{-ikj} - z + d(e^{-ikj} - 1) \right] \end{aligned} \quad (12)$$

where  $V' = V'(h)$ , making  $z = z_1(ik) + z_2(ik)^2 + \dots$ , then the first-order and second-order terms of  $ik$  are

$$z_1 = V', z_2 = \frac{1}{2} V' - \tau_1 V'^2 + \tau \lambda V' + \frac{k_1 d \tau}{c} \sum_{j=1}^m j w_j - \tau V'^2 \quad (13)$$

According to the long wave theory, if  $z_2 > 0$ , traffic flow reaches a steady state. Otherwise, the traffic flow is unstable. The condition for unstable traffic flow is

$$\tau > \frac{\frac{1}{2} - \tau_1 V'}{\lambda + \frac{k_1 d}{c} \sum_{j=1}^m j w_j - V'} \quad (14)$$

This result is related to  $k_1$  and  $\tau_1$ . The neutral stable lines of the proposed model considering the electronic throttle and driver's memory effect are shown in Figure 1 with  $v_{\max} = 2$ ,  $h_c = 4$ . The apex of each neutral stability curve is the critical point  $(h_c, \alpha_c)$ . For a given neutral stability curve, the region above the curve is the stable region, and the region below the curve is the unstable region, and uniform traffic flow should become unstable in this region.

Pattern (a) of Figure 1 demonstrates that when the value of  $\tau_1$  is increased, the neutral line decreases and the stable region gradually decreases, indicating that the memory effect gradually weakens the stability of the traffic flow. Therefore, the memory effect of the driver plays a negative role in enhancing the stability of traffic flow.

Pattern (b) of Figure 1 shows that as the  $k_1$  increases, the neutral curve gradually decreases and the stable region gradually expands, indicating that the electronic throttle effect has an important role in improving the stability of traffic flow.

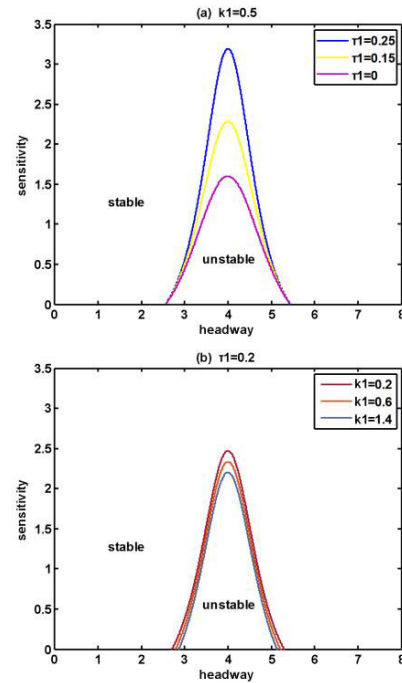


FIGURE 1. The neutral stability curves for different values of  $\tau_1$  and  $k_1$ .

### B. THE TDGL EQUATION

The nonlinear density wave equation is used to describe the phase change behavior of traffic jams, We discover traffic problems through nonlinear analysis and adopt methods to solve them, The TDGL equation for evolution of density wave is derived by reduced perturbation method. First, introduce the slow variables of space  $n$  and time  $t$ , as defined below

$$X = \varepsilon(n + bt) \quad T = \varepsilon^3 t \quad 0 < \varepsilon \leq 1 \quad (15)$$

The headway  $\Delta x_n$  is set as

$$\Delta x_n(t) = h_c + \varepsilon R(X, T) \quad (16)$$

$$\begin{aligned} \varepsilon^2 \xi_1 \partial_x R + \varepsilon^3 \xi_2 \partial_x^2 R \\ + \varepsilon^4 \left[ \xi^3 \partial_x^3 R + \xi^4 \partial_x R^3 - a \partial_T R \right] \\ + \varepsilon^5 \left[ \xi^5 \partial_x^4 R + \xi^6 \partial_x \partial_T R + \xi^7 \partial_x^2 R^3 \right] = 0 \end{aligned} \quad (17)$$

where the coefficients  $\xi_i$  are given in Table 1.

Then, we study traffic flow near the critical point  $(h_c, \alpha_c)$ , making  $b = V'$ ,  $\alpha_c = (1 + \varepsilon^2)\alpha$ , the second-order terms of  $\varepsilon$  is removed from Eq. (16), the equation can be simplified to

$$\begin{aligned} \varepsilon^4 \partial_T R \\ = \varepsilon^4 \left[ \frac{1}{6} V' - \frac{1}{2} \tau_1 V'^2 + \frac{1}{2} \lambda V' \tau \right. \\ \left. + \left( \frac{V'^2 k_1}{c} \sum_{j=1}^m w_{jj} - \frac{dV' k_1}{2c} \sum_{j=1}^m w_{jj} \right) \frac{1 - 2\tau_1 V'}{c} \sum_{j=1}^m w_{jj} \right] \partial_x^3 R \\ + \varepsilon^3 \left[ \frac{1}{2} V' - \tau_1 V'^2 + \left( \frac{k_1 d}{c} \sum_{j=1}^m w_{jj} - V' \right) V' \tau + \lambda V' \tau \right] \partial_x^2 R \end{aligned}$$

TABLE 1. The coefficient  $\xi_i$  of the model.

$\xi_1$	$\alpha(V' - b)$
$\xi_2$	$\frac{1}{2}\alpha V' - b^2 - ab\tau_1 V' + \frac{k_1 db}{c} \sum_{j=1}^m w_{j,j} + \lambda b$
$\xi_3$	$\frac{1}{6}\alpha V' - \frac{1}{2}\alpha b\tau_1 V' + \frac{k_1 b^2}{c} \sum_{j=1}^m w_{j,j} - \frac{1}{2} \frac{k_1 db}{c} \sum_{j=1}^m w_{j,j}^2 + \frac{1}{2}\lambda b$
$\xi_4$	$\frac{1}{6} aV''''$
$\xi_5$	$\frac{1}{24}\alpha - \frac{ab\tau_1 V'}{6} - \frac{k_1 b^2}{2c} \sum_{j=1}^m w_{j,j}^2 + \frac{1}{6}\lambda b$
$\xi_6$	$\alpha\tau_1 V' - 2b + \frac{k_1 d}{c} \sum_{j=1}^m w_{j,j}$
$\xi_7$	$\frac{1}{2} \alpha V''''$

$$\begin{aligned}
 & + \varepsilon^5 \left[ \begin{aligned} & \frac{1}{24} - \frac{\tau_1 V'^2}{6} + \frac{1}{6} \lambda V' \tau \\ & - \left( \frac{k_1 V'^2}{2c} \sum_{j=1}^m w_{j,j}^2 + \frac{k_1 d V'}{6c} \sum_{j=1}^m w_{j,j}^3 \right) \frac{1 - 2\tau_1 V'}{2k_1 d \sum_{j=1}^m w_{j,j}} \end{aligned} \right] \\
 & \times \partial_x^4 R \\
 & + \varepsilon^4 \frac{V''''}{6} \partial_x R^3 + \varepsilon^5 \frac{V''''}{2} \partial_x^2 R^3 \tag{18}
 \end{aligned}$$

By transforming variables  $X$  and  $T$  to variables  $x = \varepsilon^{-1}X$  and  $t = \varepsilon^{-3}T$ , and taking  $S(x, t) = \varepsilon R(X, T)$ , Eq. (18) is rewritten as follows

$$\begin{aligned}
 \partial_t R & = \left[ \begin{aligned} & \frac{1}{6} V' - \frac{1}{2} \tau_1 V'^2 + \frac{1}{2} \lambda V' \tau + \\ & \left( \frac{V'^2}{c} \sum_{j=1}^m w_{j,j} - \frac{k_1 d V'}{2c} \sum_{j=1}^m w_{j,j}^2 \right) \frac{1 - 2\tau_1 V'}{2k_1 d \sum_{j=1}^m w_{j,j}} \end{aligned} \right] \partial_x^3 S \\
 & + \left[ \begin{aligned} & \frac{1}{2} V' - \tau_1 V'^2 + \left( \frac{k_1 d}{c} \sum_{j=1}^m w_{j,j} - V' \right) V' \tau + \lambda V' \tau \end{aligned} \right] \partial_x^2 S \\
 & + \frac{V''''}{2} \partial_x^2 S^3 + \frac{V''''}{6} \partial_x S^3 \\
 & + \left[ \begin{aligned} & \frac{1}{24} - \frac{\tau_1 V'^2}{6} + \frac{1}{6} \lambda V' \tau \\ & - \left( \frac{k_1 V'^2}{2c} \sum_{j=1}^m w_{j,j}^2 + \frac{d k_1 V'}{6c} \sum_{j=1}^m w_{j,j}^3 \right) \frac{1 - 2\tau_1 V'}{2k_1 d \sum_{j=1}^m w_{j,j}} \end{aligned} \right] \partial_x^4 S \tag{19}
 \end{aligned}$$

By adding item  $\left[ \frac{1}{2} V' - \tau_1 V'^2 + \left( \frac{k_1 d}{c} \sum_{j=1}^m w_{j,j} - V' \right) V' \tau \right] \partial_x S$  on the left and right sides of Eq. (19) and performing  $t_1 = t$  and  $x_1 = x - \left[ \left( \frac{k_1 d}{c} \sum_{j=1}^m w_{j,j} - V' \right) V' \tau - \frac{1}{2} V' + \tau_1 V'^2 \right] t$  for Eq. (19), and we obtain, as in (20), shown at the bottom of the next page.

We define the thermodynamic potential

$$\begin{aligned}
 \phi(S) & = - \left[ \begin{aligned} & \frac{1}{2} V' - \tau_1 V'^2 + \left( \frac{k_1 d}{c} \sum_{j=1}^m w_{j,j} - V' + \lambda \right) V' \tau \end{aligned} \right] S \\
 & + \frac{V''''}{2} S^4 \tag{21}
 \end{aligned}$$

By rewriting Eq. (20) with (21), the TDGL equation for this model

$$\partial_{t_1} S = - \left( \partial_{x_1} - \frac{1}{2} \partial_{x_1}^2 \right) \frac{\delta \Phi(S)}{\delta S} \tag{22}$$

With

$$\begin{aligned}
 \Phi(S) & = \int dx_1 \\
 & \times \left\{ \left[ \begin{aligned} & \frac{1}{6} V' - \frac{1}{2} \tau_1 V'^2 + \frac{1}{2} \lambda V' \tau \\ & + \left( \frac{k_1 V'^2}{c} \sum_{j=1}^m w_{j,j} - \frac{k_1 d V'}{2c} \sum_{j=1}^m w_{j,j}^2 \right) \frac{1 - 2\tau_1 V'}{2k_1 d \sum_{j=1}^m w_{j,j}} \end{aligned} \right] \right. \\
 & \left. \times (\partial_{x_1} S)^2 + \phi(S) \right\} \tag{23}
 \end{aligned}$$

where  $\delta \Phi(S) / \delta S$  represents derivative of a function. In addition to  $S = 0$ , the TDGL equation has two steady-state solutions, one of which is a homogeneous solution

$$\begin{aligned}
 S(x_1, t_1) & = \pm \left[ \begin{aligned} & 3V' - 6\tau_1 V'^2 + 6 \left( \frac{k_1 d}{c} \sum_{j=1}^m w_{j,j} - V' + \lambda \right) V' \tau \end{aligned} \right]^{\frac{1}{2}} \\
 & \frac{V''''}{V''''} \tag{24}
 \end{aligned}$$

And the other is the kink solution

$$\begin{aligned}
 S(x_1, t_1) & = \pm \left[ \begin{aligned} & 3V' - 6\tau_1 V'^2 + 6 \left( \frac{k_1 d}{c} \sum_{j=1}^m w_{j,j} - V' + \lambda \right) V' \tau \end{aligned} \right]^{\frac{1}{2}} \\
 & \times \tanh \left\{ \left[ \begin{aligned} & \frac{1}{2} V' - \tau_1 V'^2 + \left( \frac{k_1 d}{c} \sum_{j=1}^m w_{j,j} - V' + \lambda \right) V' \tau \end{aligned} \right]^{\frac{1}{2}} \right. \\
 & \left. \times (x_1 - x_0) \right\} \tag{25}
 \end{aligned}$$

where  $x_0$  is a constant. From the thermodynamic potential equation, we can obtain the coexistence curve, the metastable curve and the critical point. The conditions that satisfy the coexistence curve are as follows

$$\partial\phi/\partial S = 0, \partial^2\phi/\partial S^2 > 0 \tag{26}$$

If we substitute Eq. (21) into Eq. (26), we get the coexistence curve with the original parameters

$$(\Delta x)_{co} = h_c \pm \left[ \frac{3V' - 6\tau_1 V'^2 + 6\left(\frac{k_1 d}{c} \sum_{j=1}^m w_{jj} - V' + \lambda\right)V'\tau}{V'''} \right]^{\frac{1}{2}} \tag{27}$$

The conditions for the critical point are as follows

$$\partial^2\phi/\partial S^2 = 0 \tag{28}$$

From Eq. (21), the metastable curve equation is obtained

$$(\Delta x)_{co} = h_c \pm \left[ \frac{V' - 2\tau_1 V'^2 + 2\left(\frac{k_1 d}{c} \sum_{j=1}^m w_{jj} - V' + \lambda\right)V'\tau}{V'''} \right]^{\frac{1}{2}} \tag{29}$$

From the above, we can get the critical point of the original parameter

$$(\Delta x)_c = h_c, a = \frac{2\lambda + \frac{2k_1 d}{c} \sum_{j=1}^m jw_j - 2V'}{1 - 2\tau_1 V'} \tag{30}$$

**C. THE mKdV EQUATION**

The mKdV equation near the critical point is derived. Similarly, near the critical point  $(h_c, \alpha_c)$ , slow variables  $X$  and  $T$  of space and time are introduced. By substituting  $\tau = (1 + \varepsilon^2)\tau_c$  into Eq. (17), we can gain

$$\varepsilon^4(\partial_T R - \zeta_1 \partial_X^3 R + \zeta_2 \partial_X R^3) + \varepsilon^5(\zeta_3 \partial_X^2 R + \zeta_4 \partial_X^2 R^3 + \zeta_5 \partial_X^4 R) = 0 \tag{31}$$

where the coefficients  $\zeta_i$  are given in Table 2.

**TABLE 2. The coefficient  $\zeta_i$  of the model.**

$\zeta_1$	$\left(\frac{k_1 V'^2}{c} \sum_{j=1}^m w_{jj} - \frac{k_1 d V'}{2c} \sum_{j=1}^m w_{jj}^2\right) \frac{1 - 2\tau_1 V'}{c \sum_{j=1}^m w_{jj}} + \frac{1}{2} V' \lambda - \frac{1}{6} V' - \frac{1}{2} \tau_1 V'^2$
$\zeta_2$	$\frac{V'''}{6}$
$\zeta_3$	$\frac{1}{2} V' + \left(\frac{k_1 d}{c} \sum_{j=1}^m w_{jj} - V' + \lambda\right) V'$
$\zeta_4$	$\frac{V'''}{2} + \tau_1 V' + \frac{d k_1}{c} \sum_{j=1}^m w_{jj} + \lambda$
$\zeta_5$	$\frac{1}{24} - \left(\frac{k_1 V'^2}{2c} \sum_{j=1}^m w_{jj}^3 + \frac{k_1 d V'}{6c} \sum_{j=1}^m w_{jj}^3\right) \frac{1 - 2\tau_1 V'}{c \sum_{j=1}^m w_{jj}} + \frac{1}{2} \lambda V' - \frac{\tau_1 V'^2}{6}$

In the table above  $V' = dV(\Delta x_n)/d\Delta x_n|_{\Delta x_n=h_c}$ ,  $V''' = d^3V(\Delta x_n)/d\Delta x_n^3|_{\Delta x_n=h_c}$ . For simplifying the derivation, let's introduce a transformation

$$T = \frac{1}{\zeta_1} T', R = \sqrt{\frac{\zeta_1}{\zeta_2}} R' \tag{32}$$

So we get an standard mKdV equation with an  $O(\varepsilon)$  correction term as follows

$$\partial_{T'} R' = \partial_X^3 R' - \partial_X R'^3 - \varepsilon \left[ \frac{\zeta_3}{\zeta_1} \partial_X^2 R' + \frac{\zeta_4}{\zeta_1} \partial_X^4 R' + \frac{\zeta_5}{\zeta_2} \partial_X^2 R'^3 \right] \tag{33}$$

If the higher order  $O(\varepsilon)$  is neglected, we can obtain a kink-antikink density wave solution of mKdV equation

$$R'_0(X, T') = \sqrt{c} \tanh \sqrt{\frac{c}{2}} (X - cT') \tag{34}$$

Assuming that  $R'(X, T') = R'_0(X, T') + \varepsilon R'_1(X, T')$ , If we consider the  $O(\varepsilon)$  correction term, the solvable condition

$$\partial_{T'} S = \left\{ \left[ \frac{1}{6} V' - \frac{1}{2} \tau_1 V'^2 + \left(\frac{k_1 V'^2}{c} \sum_{j=1}^m w_{jj} - \frac{d k_1 V'}{2c} \sum_{j=1}^m w_{jj}^2\right) \times \frac{1 - 2\tau_1 V'}{c \sum_{j=1}^m w_{jj}} + \frac{1}{2} V' \lambda \tau \right] \partial_{X_1}^2 S \times \left(\partial_{X_1} - \frac{1}{2} \partial_{X_1}^2\right) \times - \left[ \frac{1}{2} V' - \tau_1 V'^2 + \left(\frac{k_1 d}{c} \sum_{j=1}^m w_{jj} - V'\right) V' \tau + \lambda V' \tau \right] S - \frac{V'''}{2} S^3 \right\} \tag{20}$$

$(R'_0, M[R']) \equiv \int_{-\infty}^{+\infty} dX' R'_0 M[R']$  can be used. where  $M[R'_0] = \frac{\zeta_3}{\zeta_1} \partial_X^2 R' + \frac{\zeta_4}{\zeta_1} \partial_X^4 R' + \frac{\zeta_5}{\zeta_2} \partial_X^2 R'^3$ , Therefore, the propagation velocity  $c$  of the kink wave can be determined

$$c = \frac{5\zeta_2\zeta_3}{2\zeta_2\zeta_4 - 3\zeta_1\zeta_5} \quad (35)$$

The general kinking solution of the mKdV equation is

$$\Delta x_n(t) = h_c \pm \sqrt{\frac{\zeta_1 c}{\zeta_2} \left(\frac{\tau}{\tau_c} - 1\right)} \times \tanh \sqrt{\frac{c}{2} \left(\frac{\tau}{\tau_c} - 1\right)} \times \left[ n + (1 - c\zeta_1) \left(\frac{\tau}{\tau_c} - 1\right) t \right] \quad (36)$$

where  $V''' < 0$ , the kink solution includes the coexistence phase of the free phase at low density and the coexistence phase of blocked phase at high density. The kink solution of the mKdV equation (36) coincides with the kink solution of the TDGL equation (25), which indicates that the phase transition behavior of the plugged phase can be described not only by TDGL equation and its non-travelling wave solution, but also by mKdV equation and propagation solution.

### III. RESULTS AND DISCUSSION

#### A. NUMERICAL SIMULATION

The effects of driver's memory and electronic throttle on the car following model are studied by numerical simulation. Equation (4) is discretized by difference scheme

$$\begin{aligned} &\Delta x_n(t + 2\Delta t) \\ &= 2\Delta x_n(t + \Delta t) - \Delta x_n(t) \\ &\quad + \alpha \Delta t^2 (V(\Delta x_{n+1}(t)) - V(\Delta x_n(t))) \\ &\quad - \alpha \tau_1 V' \Delta t (\Delta x_{n+1}(t + \Delta t) - \Delta x_n(t)) \\ &\quad - \Delta x_n(t + \Delta t) + \Delta x_n(t) \\ &\quad - \alpha \Delta t (\Delta x_n(t + \Delta t) - \Delta x_n(t)) \\ &\quad + \lambda \Delta t (\Delta x_{n+1}(t + \Delta t) - \Delta x_{n+1}(t)) \\ &\quad - \Delta x_n(t + \Delta t) + \Delta x_n(t) + \frac{k_1}{c} \sum_{j=1}^m w_j (\Delta x_n(t + 2\Delta t) \\ &\quad - 2\Delta x_n(t + \Delta t) + \Delta x_n(t)) \\ &\quad - \Delta x_{n-j}(t + 2\Delta t) + 2\Delta x_{n-j}(t + \Delta t) - \Delta x_{n-j}(t)) \\ &\quad + \Delta t \frac{k_1 d}{c} \sum_{j=1}^m w_j (\Delta x_n(t + \Delta t) \\ &\quad - \Delta x_n(t) - \Delta x_{n-j}(t + \Delta t) + \Delta x_{n-j}(t)) \end{aligned} \quad (37)$$

where  $\Delta t$  is the time step, the boundary condition is chosen to be periodic and  $h_c = 4m$ . In the numerical simulation, we selected  $n = 3$  and obtained a CAV vehicle following model with three front car electronic throttle controls for numerical simulation experiments. The initial condition is chosen as follows

$$\Delta x_n(t) = \Delta x_n(0), \Delta x_n(0) = \begin{cases} h & n \neq 50, 51 \\ h - 0.5 & n = 50 \\ h + 0.5 & n = 51 \end{cases} \quad (38)$$

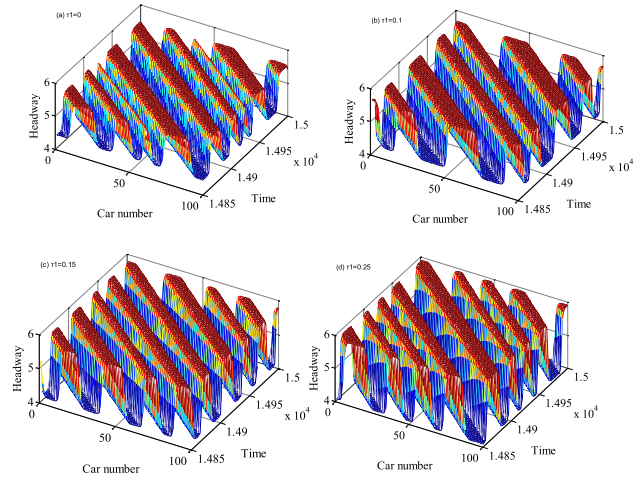


FIGURE 2. The spatial-time evolutions of the headway from  $t = 14850$  to  $15000$  sec for different values of  $\tau_1$ .

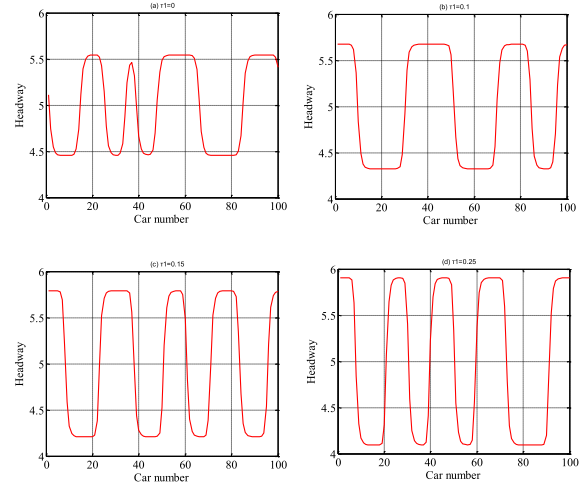


FIGURE 3. The headway profiles of density wave at  $t = 15000$  sec for different values of  $\tau_1$ .

where  $N = 100$  is the number of cars,  $h$  is the average headway.

#### B. THE INFLUENCE OF DRIVER'S MEMORY EFFECT ON TRAFFIC FLOW STABILITY

First, we will examine the impact of parameter  $\tau_1$  on the stability of traffic flow. Figure 2 shows the space and time evolution of the headway for vehicles with different value of  $\tau_1$ . When  $\tau_1 = 0$  in pattern (a), the evolution of the traffic flow in the extended model without memory effect. When the driver's memory effect factor is taken into consideration, as the  $\tau_1$  increases, the amplitude of the traffic flow is gradually increased, and the traffic flow becomes more and more disordered.

Fig. 3 plots the headway distribution corresponding to the time  $t = 15000$  seconds of Fig. 2, as the  $\tau_1$  increases, the amplitude of the density wave gradually increases. The

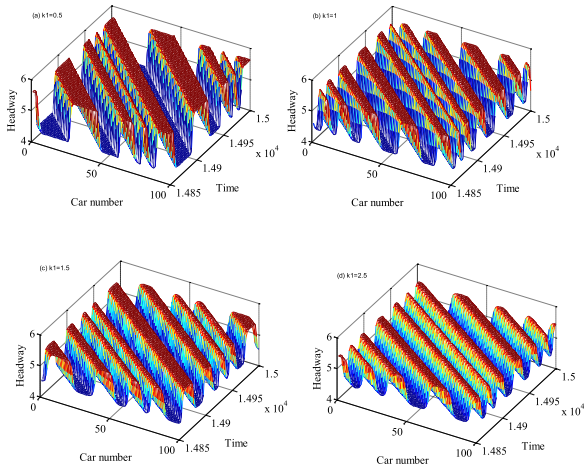


FIGURE 4. The spatial-time evolutions of the headway from  $t = 14850$  to  $15000$  sec for different values of  $k_1$ .

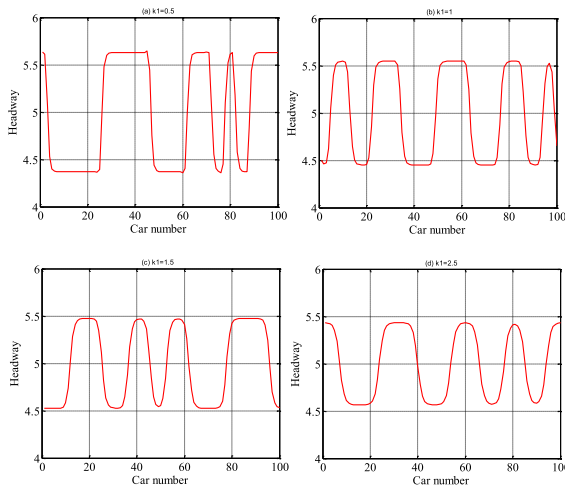


FIGURE 5. The headway profiles of density wave at  $t = 15000$  sec for different values of  $k_1$ .

driver's memory effect has a reverse effect on the stability of traffic flow in the model.

### C. THE INFLUENCE OF ELECTRONIC THROTTLE ON TRAFFIC FLOW STABILITY

In order to study the influence of the electronic throttle coefficient  $k_1$ , the memory effect coefficient is fixed to be  $\tau_1 = 0.5$ . And for  $k_1 = 0.5, 1, 1.5, 2.5$ , the headway distribution at  $t = 15000$  seconds along the road is shown in Figure 4. With the increase of  $k_1$ , the amplitude of the density wave decreases gradually, and the traffic jam is alleviated well. It can be seen that within a certain range, the value of  $k_1$  should be as large as possible to enhance the stability of traffic flow to a certain extent.

Figure 5 depicts the change of headway for different values of  $k_1 = 0.5, 1, 1.5, 2.5$ , corresponding to Figure 4. It can be seen from the figure that increasing the value of electronic throttle coefficient  $k_1$  can reduce traffic congestion and improve the stability of the traffic flow.

### IV. CONCLUSION

Considering the memory effect of the driver and the effect of the electronic throttle on the traffic jam, we have studied an extended model. In order to show the effect of memory and the effect of electronic throttle on traffic congestion, the extended model was studied by theoretical analysis and numerical methods. The stability conditions of the new model are obtained by linear analysis. Then, by using the nonlinear analysis method, the TDGL equation and the modified KdV equation are derived, The phase transition behavior of the blocked phase can be described by TDGL equation and mKdV equation. Theoretical analysis and numerical results show that the memory effect of the driver and the electronic throttle have an important influence on the stability of traffic flow.

The main findings of the paper are as follows:

First, we will examine the impact of driver's memory effect on the stability of traffic flow. When  $\tau_1 = 0$ , the evolution of the traffic flow in the extended model without memory effect. When the driver's memory effect factor is taken into consideration, as the  $\tau_1$  increases, the amplitude of the traffic flow is gradually increased, and the traffic flow becomes more and more disordered.

Secondly, in order to study the influence of the electronic throttle coefficient, with the increase of  $k_1$ , the amplitude of the density wave gradually decreases, and the consideration of electronic throttle has a great improvement on traffic congestion.

In conclusion, The driver's memory effect and the electronic throttle effect effectively alleviate traffic congestion and reduce carbon emissions.

### REFERENCES

- [1] Y. Li, X. Lu, C. Ren, and H. Zhao, "Fusion modeling method of car-following characteristics," *IEEE Access*, vol. 7, pp. 162778–162785, 2019.
- [2] R. Cheng, H. Ge, and J. Wang, "An extended macro traffic flow model accounting for multiple optimal velocity functions with different probabilities," *Phys. Lett. A*, vol. 381, no. 32, pp. 2608–2620, Aug. 2017.
- [3] Z. Wen-Xing and Z. Li-Dong, "A new car-following model for autonomous vehicles flow with mean expected velocity field," *Phys. A, Stat. Mech. Appl.*, vol. 492, pp. 2154–2165, Feb. 2018.
- [4] S. Yu, J. Tang, and Q. Xin, "Relative velocity difference model for the car-following theory," *Nonlinear Dyn.*, vol. 91, no. 3, pp. 1415–1428, Feb. 2018.
- [5] T.-Q. Tang, J. Zhang, and K. Liu, "A speed guidance model accounting for the driver's bounded rationality at a signalized intersection," *Phys. A, Stat. Mech. Appl.*, vol. 473, pp. 45–52, May 2017.
- [6] W.-X. Zhu and H. M. Zhang, "Analysis of mixed traffic flow with human-driving and autonomous cars based on car-following model," *Phys. A, Stat. Mech. Appl.*, vol. 496, pp. 274–285, Apr. 2018.
- [7] H. Ou and T.-Q. Tang, "An extended two-lane car-following model accounting for inter-vehicle communication," *Phys. A, Stat. Mech. Appl.*, vol. 495, pp. 260–268, Apr. 2018.
- [8] C. Ma, W. Hao, R. He, X. Jia, F. Pan, J. Fan, and R. Xiong, "Distribution path robust optimization of electric vehicle with multiple distribution centers," *PLoS ONE*, vol. 13, no. 3, Mar. 2018, Art. no. e0193789.
- [9] M. Abdollahzade and R. Kazemi, "An intelligent evolving car-following model," *IEEE Access*, vol. 11, pp. 506–516, 2023.
- [10] C. Ma, W. Hao, F. Pan, and W. Xiang, "Road screening and distribution route multi-objective robust optimization for hazardous materials based on neural network and genetic algorithm," *PLoS ONE*, vol. 13, no. 6, Jun. 2018, Art. no. e0198931.

- [11] Q. Xin, N. Yang, R. Fu, S. Yu, and Z. Shi, "Impacts analysis of car following models considering variable vehicular gap policies," *Phys. A, Stat. Mech. Appl.*, vol. 501, pp. 338–355, Jul. 2018.
- [12] C. Ma, R. He, and W. Zhang, "Path optimization of taxi carpooling," *PLoS ONE*, vol. 13, no. 8, Aug. 2018, Art. no. e0203221.
- [13] T.-Q. Tang, X.-F. Luo, J. Zhang, and L. Chen, "Modeling electric bicycle's lane-changing and retrograde behaviors," *Phys. A, Stat. Mech. Appl.*, vol. 490, pp. 1377–1386, Jan. 2018.
- [14] H. Ou, T.-Q. Tang, J. Zhang, and J.-M. Zhou, "A car-following model accounting for probability distribution," *Phys. A, Stat. Mech. Appl.*, vol. 505, pp. 105–113, Sep. 2018.
- [15] C. Ma, W. Hao, A. Wang, and H. Zhao, "Developing a coordinated signal control system for urban ring road under the vehicle-infrastructure connected environment," *IEEE Access*, vol. 6, pp. 52471–52478, 2018.
- [16] C. Zhai and W. Wu, "A new car-following model considering driver's characteristics and traffic jerk," *Nonlinear Dyn.*, vol. 93, no. 4, pp. 2185–2199, Sep. 2018.
- [17] Y. Li, H. Zhao, L. Zhang, and C. Zhang, "An extended car-following model incorporating the effects of lateral gap and gradient," *Phys. A, Stat. Mech. Appl.*, vol. 503, pp. 177–189, Aug. 2018.
- [18] C. Jiang, R. Cheng, and H. Ge, "An improved lattice hydrodynamic model considering the 'backward looking' effect and the traffic interruption probability," *Nonlinear Dyn.*, vol. 91, no. 2, pp. 777–784, Jan. 2018.
- [19] C. Jiang, R. Cheng, and H. Ge, "Mean-field flow difference model with consideration of on-ramp and off-ramp," *Phys. A, Stat. Mech. Appl.*, vol. 513, pp. 465–476, Jan. 2019.
- [20] G. Peng, H. Kuang, H. Zhao, and L. Qing, "Nonlinear analysis of a new lattice hydrodynamic model with the consideration of honk effect on flux for two-lane highway," *Phys. A, Stat. Mech. Appl.*, vol. 515, pp. 93–101, Feb. 2019.
- [21] J. Wang, F. Sun, and H. Ge, "An improved lattice hydrodynamic model considering the driver's desire of driving smoothly," *Phys. A, Stat. Mech. Appl.*, vol. 515, pp. 119–129, Feb. 2019.
- [22] T.-Q. Tang, Y.-X. Rui, J. Zhang, and H.-Y. Shang, "A cellular automation model accounting for bicycle's group behavior," *Phys. A, Stat. Mech. Appl.*, vol. 492, pp. 1782–1797, Feb. 2018.
- [23] Y. Zhang and S.-G. Li, "Multi-fractal analysis for vehicle distribution based on cellular automation model," *Mod. Phys. Lett. B*, vol. 29, no. 26, Sep. 2015, Art. no. 1550153.
- [24] R. Cheng, H. Ge, and J. Wang, "KdV–Burgers equation in a new continuum model based on full velocity difference model considering anticipation effect," *Phys. A, Stat. Mech. Appl.*, vol. 481, pp. 52–59, Sep. 2017.
- [25] Z. Qingtao, G. Hongxia, and C. Rongjun, "An extended continuum model considering optimal velocity change with memory and numerical tests," *Phys. A, Stat. Mech. Appl.*, vol. 490, pp. 774–785, Jan. 2018.
- [26] R. J. Cheng, H. X. Ge, and J. F. Wang, "The nonlinear analysis for a new continuum model considering anticipation and traffic jerk effect," *Appl. Math. Comput.*, vol. 332, pp. 493–505, Jan. 2018.
- [27] R. Cheng, H. Ge, and J. Wang, "An extended continuum model accounting for the driver's timid and aggressive attributions," *Phys. Lett. A*, vol. 381, no. 15, pp. 1302–1312, Apr. 2017.
- [28] M. Bando, K. Hasebe, A. Nakayama, A. Shibata, and Y. Sugiyama, "Dynamical model of traffic congestion and numerical simulation," *Phys. Rev. E, Stat. Phys. Plasmas Fluids Relat. Interdiscip. Top.*, vol. 51, no. 2, pp. 1035–1042, Feb. 1995.
- [29] T. Nagatani, "Gas kinetics of traffic jam," *J. Phys. Soc. Jpn.*, vol. 66, no. 4, pp. 1219–1224, Apr. 1997.
- [30] T. Nagatani, "Gas kinetic approach to two-dimensional traffic flow," *J. Phys. Soc. Jpn.*, vol. 65, no. 10, pp. 3150–3152, Oct. 1996.
- [31] M. Treiber, A. Hennecke, and D. Helbing, "Derivation, properties, and simulation of a gas-kinetic-based, nonlocal traffic model," *Phys. Rev. E, Stat. Phys. Plasmas Fluids Relat. Interdiscip. Top.*, vol. 59, no. 1, pp. 239–253, Jan. 1999.
- [32] D. Helbing and B. Tilch, "Generalized force model of traffic dynamics," *Phys. Rev. E, Stat. Phys. Plasmas Fluids Relat. Interdiscip. Top.*, vol. 58, no. 1, pp. 133–138, Jul. 1998.
- [33] R. Jiang, Q. Wu, and Z. Zhu, "Full velocity difference model for a car-following theory," *Phys. Rev. E, Stat. Phys. Plasmas Fluids Relat. Interdiscip. Top.*, vol. 64, no. 1, Jun. 2001, Art. no. 017101.
- [34] G. H. Peng, X. H. Cai, C. Q. Liu, B. F. Cao, and M. X. Tuo, "Optimal velocity difference model for a car-following theory," *Phys. Lett. A*, vol. 375, no. 45, pp. 3973–3977, Oct. 2011.
- [35] Z. Li, Q. Qin, W. Li, S. Xu, Y. Qian, and J. Sun, "Stabilization analysis and modified KdV equation of a car-following model with consideration of self-stabilizing control in historical traffic data," *Nonlinear Dyn.*, vol. 91, no. 2, pp. 1113–1125, Jan. 2018.
- [36] Y. Rong and H. Wen, "An extended delayed feedback control method for the two-lane traffic flow," *Nonlinear Dyn.*, vol. 94, no. 4, pp. 2479–2490, Dec. 2018.
- [37] G. Peng, S. Yang, D. Xia, and X. Li, "Impact of lattice's self-anticipative density on traffic stability of lattice model on two lanes," *Nonlinear Dyn.*, vol. 94, no. 4, pp. 2969–2977, Dec. 2018.
- [38] H. X. Ge, S. Q. Dai, and L. Y. Dong, "An extended car-following model based on intelligent transportation system application," *Phys. A, Stat. Mech. Appl.*, vol. 365, no. 2, pp. 543–548, Jun. 2006.
- [39] Z.-P. Li and Y.-C. Liu, "Analysis of stability and density waves of traffic flow model in an ITS environment," *Eur. Phys. J. B*, vol. 53, no. 3, pp. 367–374, Oct. 2006.
- [40] L. Yu, Z. Shi, and B. Zhou, "Kink–antikink density wave of an extended car-following model in a cooperative driving system," *Commun. Nonlinear Sci. Numer. Simul.*, vol. 13, no. 10, pp. 2167–2176, Dec. 2008.
- [41] Y. Sun, H. Ge, and R. Cheng, "An extended car-following model under V2V communication environment and its delayed-feedback control," *Phys. A, Stat. Mech. Appl.*, vol. 508, pp. 349–358, Oct. 2018.
- [42] S. Yu and Z. Shi, "The effects of vehicular gap changes with memory on traffic flow in cooperative adaptive cruise control strategy," *Phys. A, Stat. Mech. Appl.*, vol. 428, pp. 206–223, Jun. 2015.
- [43] B.-G. Cao, "A new car-following model considering driver's sensory memory," *Phys. A, Stat. Mech. Appl.*, vol. 427, pp. 218–225, Jun. 2015.
- [44] Y. Li, H. Zhao, T. Zheng, F. Sun, and H. Feng, "Non-lane-discipline-based car-following model incorporating the electronic throttle dynamics under connected environment," *Nonlinear Dyn.*, vol. 90, no. 4, pp. 2345–2358, Dec. 2017.
- [45] Y. Li, L. Zhang, S. Peeta, X. He, T. Zheng, and Y. Li, "A car-following model considering the effect of electronic throttle opening angle under connected environment," *Nonlinear Dyn.*, vol. 85, no. 4, pp. 2115–2125, Sep. 2016.
- [46] G. Peng, F. Nie, B. Cao, and C. Liu, "A driver's memory lattice model of traffic flow and its numerical simulation," *Nonlinear Dyn.*, vol. 67, no. 3, pp. 1811–1815, Feb. 2012.



**CHEN CAN** was born in Hubei, China. She is currently pursuing the Ph.D. degree with the School of Transportation, Wuhan University of Technology. She is also studying with Nanyang Technological University, Singapore. Her current research interests include intelligent transportation systems and public transportation operation management.



**DU ZHIGANG** received the Ph.D. degree. He is currently a Professor with the Department of Transportation Engineering, Wuhan University of Technology, and a Ph.D. Supervisor. He has been engaged in teaching and research work in road traffic safety and environment, and traffic engineering facilities for a long time. He is with the leading domestic level in tunnel traffic safety research.